

SCALAR MESON PAIRS IN NUCLEI
EXPERIMENTAL RESULTS*

N. GRION

for the CHAOS collaboration

Istituto Nazionale di Fisica Nucleare
34127 Trieste, Italy*(Received June 15, 2000)*

The $\pi^+A \rightarrow \pi^+\pi^\pm A'$ reactions were studied on ^2H , ^{12}C , ^{40}Ca and ^{208}Pb nuclei at $T_{\pi^+} = 283$ MeV. Pions were detected in coincidence using the CHAOS spectrometer. The composite ratio $\mathcal{C}_{\pi\pi}^A$ between the $\pi^+\pi^\pm$ invariant masses on nuclei and on the nucleon is presented. Near the $2m_\pi$ threshold pion pairs couple to $(\pi\pi)_{I=J=0}$ when produced in the $\pi^+ \rightarrow \pi^+\pi^-$ reaction channel. There is a marked near-threshold enhancement of $\mathcal{C}_{\pi^+\pi^-}^A$ which is consistent with theoretical predictions addressing the partial restoration of chiral symmetry in nuclear matter. On the other hand, nuclear matter only weakly influences $\mathcal{C}_{\pi^+\pi^+}^A$, which displays a flat behaviour throughout the energy range regardless of A .

PACS numbers: 25.80.Hp

1. Introduction

The influence of the nuclear medium on the $\pi\pi$ interaction was investigated at TRIUMF using the pion induced pion-production reactions $\pi^+A \rightarrow \pi^+\pi^\pm A'$ (henceforth labelled $\pi 2\pi$). The initial study was directed to the reactions in deuterium, that is, to $\pi^+n(p) \rightarrow \pi^+\pi^-p(p)$ and $\pi^+p(n) \rightarrow \pi^+\pi^+n(n)$, in order to understand the $\pi 2\pi$ behaviour on both a neutron and a proton through quasi-free reactions. The $\pi 2\pi$ process was then examined on the complex nuclei ^{12}C , ^{40}Ca and ^{208}Pb in order to study possible $\pi\pi$ medium modifications by direct comparison of the $\pi 2\pi$ data. To ensure the validity of this approach, the following experimental method was applied. All the $\pi 2\pi$ data were taken under the same kinematical conditions. The

* Presented at the Meson 2000, Sixth International Workshop on Production, Properties and Interaction of Mesons, Cracow, Poland, May 19–23, 2000.

final $\pi^+\pi^\pm$ pairs were detected in coincidence to ensure a reliable identification of $\pi 2\pi$ events. Pion pairs were analysed down to 0° $\pi\pi$ opening angles to determine the $\pi\pi$ invariant mass at the $2m_\pi$ threshold. The energy of the incident pion beam, $T_{\pi^+} = 283$ MeV, was chosen to enable the investigation of the $\pi A \rightarrow \pi\pi A'$ reaction in the near-threshold region.

Some $\pi 2\pi$ articles were recently published by the CHAOS collaboration at TRIUMF. The data highlighted some properties of the in-vacuum $\pi\pi$ interaction [1–3], as well as the in-medium modifications of the $\pi\pi$ interaction [4–6]. The appearance of the CHAOS results have renewed theoretical interest, which now bases the interpretation of the $\pi 2\pi$ and $\pi\pi$ data on some common features:

1. The $\pi\pi$ interaction is strongly influenced and modified by the presence of the nuclear medium when the $\pi\pi$ interaction occurs in the $(\pi\pi)_{I=J=0}$ channel, conventionally called the σ -channel [7–10].
2. Nuclear matter affects the $(\pi\pi)_{I=2,J=0}$ interaction only weakly [9,11].
3. Models which only include standard many-body correlations, *i.e.* the P -wave coupling of π 's to p - h and Δ - h configurations, are able to explain part of the observed $M_{\pi^+\pi^-}^A$ yield near the $2m_\pi$ threshold [7,9,11].

In recent theoretical works on the $(\pi\pi)_{I=J=0}$ interaction in nuclear matter [12], the effects of standard many-body correlations have been combined with those derived from the restoration of chiral symmetry in nuclear matter. The resulting $M_{\pi^+\pi^-}^A$ distributions regain strength near the $2m_\pi$ threshold as A (thus the average nuclear density ρ) increases. Such behaviour was outlined in some earlier theoretical works, which demonstrated that the $M_{\pi^+\pi^-}^A$ enhancement near threshold is a distinct consequence of the partial restoration of the chiral symmetry at $\rho < \rho_n$, the nuclear saturation density [10].

2. The experiment

The experiment was carried out at the TRIUMF Meson Facility. The M11 pion beam line transported the 282.7 MeV positive pions to the final focus which was located at the centre of the CHAOS spectrometer. CHAOS is a magnetic spectrometer which was designed for the detection of multi-particle events in the medium-energy range [13]. The magnetic field is generated by a dipole whose pole tip is 66 cm in diameter. There is a 12 cm bore at the centre for the insertion of targets, which were solid self-supporting plates of ^{12}C (0.332 g/cm 2), ^{40}Ca (0.180 g/cm 2) and ^{208}Pb (0.604 g/cm 2), and a vessel for the liquid deuterium (H: 5 cm, ϕ : 5 cm). Fig. 1 illustrates a reconstructed $\pi_i^+ \rightarrow \pi^+\pi^-p$ event on ^{12}C , and shows the geometrical dispo-

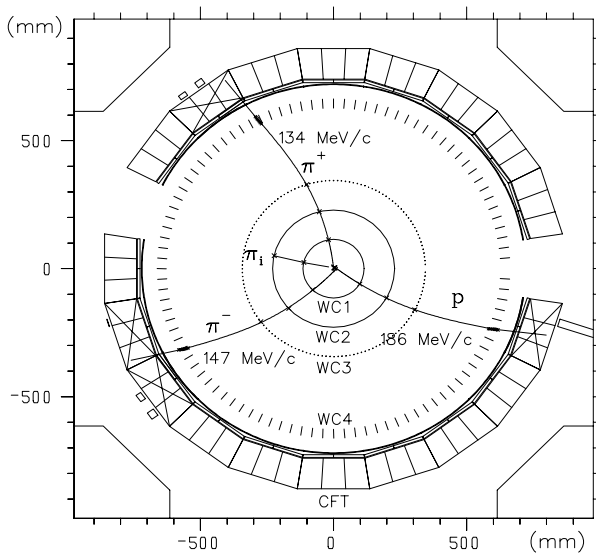


Fig. 1. Reconstructed particle trajectories in CHAOS for the $\pi_i^+ \rightarrow \pi^+ \pi^- p$ reaction on ^{12}C , the geometrical disposition of the wire chambers (WC), the first level trigger hardware (CFT) and the magnet return yokes in the corners.

sition of the Wire Chambers (WC), the CHAOS first level trigger hardware (CFT), and the magnet return yokes in the corners. The CFT hardware consists of three adjacent cylindrical layers of fast-counting detectors [14]. The first two layers ($\Delta E1$ and $\Delta E2$) are NE110 plastic scintillators 0.3 cm and 1.2 cm thick, respectively. $\Delta E1$ is 72 cm from the magnet centre and spans a zenithal angle of $\pm 7^\circ$; thus, it defines the geometrical solid angle of CHAOS $\Omega = 1.5$ sr. The third layer is a SF5 lead-glass 12.5 cm thick, about 5 radiation lengths, which is used as a Cerenkov counter. For the pion-production experiment, the CHAOS momentum resolution is $\sim 4\%$ (σ) for 130 MeV/c pions. The field (0.5 T) and the energy deposited by the particles emerging from the target in the WC's and $\Delta E1$ media determined the CHAOS threshold, which was 57 MeV/c for pions. The CHAOS acceptance is irregular in the (p_π, Θ_π) plane due to the finite segmentation of the CFT, the two missing CFT segments, and the pion decays inside CHAOS. All these sources of non-uniformity were accounted for by assigning a *weight* to each $\pi \rightarrow \pi\pi$ event. The weights were determined using GEANT Monte Carlo simulations, as described in more detail in Ref. [1].

In the case of pion-production studies, pions must be selectively separated from other reaction byproducts, essentially from e, p and d , because $\sigma_{\pi 2\pi}^A$ is from 2 to 3 orders of magnitude lower than the cross section of other competing reactions, as for instance, the quasi-elastic scattering and the

pion absorption processes. For the single charge exchange, the background arises from the $\pi^0 \rightarrow \gamma\gamma$ decay followed by the γ conversion $\gamma \rightarrow e^+e^-$. In this case the e^+e^- pair may emulate a $\pi^+\pi^-$ pair. Particles were identified by combining the information provided by WC's (particle momentum and polarity) and CFT's (pulse heights). For reactions with protons (deuterons) in the final state, *i.e.* qes and abs, the particle separation was easily achieved through the different response function of $\Delta E1$ and $\Delta E2$ to π 's and p's (d's). However, the same method of particle separation could not successfully be applied to π 's and e 's for momenta exceeding 140 MeV/ c . Thus, Cerenkov counters were used. These counters were capable of separating π 's from e 's with an efficiency of about 98% for particle momenta below 210 MeV/ c [14] Fig. 11. Finally, the π to p and e discrimination turned out to be 100% when the following soft kinematic cuts were applied to particle momenta and angles:

- Protons which passed the pion PH test were definitively rejected by restricting their momenta below 210 MeV/ c , the maximum momentum available to pions.
- Electron pairs, which might emulate $\pi^+\pi^-$ pairs, appeared with opening angles $< 2^\circ$. Therefore a 2° cut was applied during the analysis.

3. Models of the $\pi 2\pi$ reaction and the $\pi\pi$ interaction in the nuclear medium

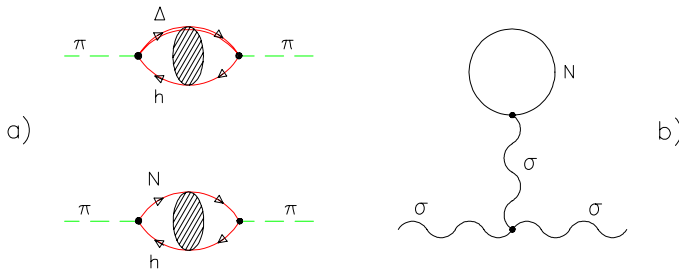


Fig. 2. Diagrams depicting a) the P -wave coupling of pions to p - h and Δ - h correlated states and b) the S -wave coupling of σ to the nuclear medium.

Before discussing the data and the comparison with the available models for both the $\pi 2\pi$ reaction and the behaviour of a $\pi\pi$ interacting system in nuclear matter, some details of the models are presented below.

(1) $\mathcal{M}1$: In order to understand the main features of medium modification on the $\pi\pi$ interacting system [11], the pion-production reaction on nuclei is modelled by means of the two leading reactions: (i) one-pion exchange $\pi^+N \rightarrow \pi^+\pi^\pm N$, which contributes to both the isoscalar and isotensor channels, and (ii) N^* excitation $\pi^+N \rightarrow N^* \rightarrow N(\pi\pi)_{I=J=0}$. The in-vacuum $\pi\pi$ interaction is accounted for by the chirally-improved Jülich model [15]. The S -wave $\pi\pi$ (final state) interaction is modified in the nuclear medium through standard renormalization of the pion propagator (see Fig. 2(a)) which determines the following: in the $\pi^+\pi^-$ channel, the isoscalar $\pi\pi$ amplitude is strongly reshaped which finally provides the near-threshold $M_{\pi^+\pi^-}$ enhancement observed in the CHAOS data; in the $\pi^+\pi^+$ channel, the nuclear density has little effect on the pure isotensor $\pi\pi$ amplitude. In order to have a realistic comparison with the CHAOS results, the model deals with Fermi motion and pion absorption although using approximate approaches, and calculates the many-fold differential cross sections by accounting for the CHAOS acceptance.

(2) $\mathcal{M}2$: The effort in Ref. [9] is to model the $\pi^+A \rightarrow \pi^+\pi^\pm A'$ reaction through a microscopic description of the elementary $\pi N \rightarrow \pi\pi N$ reaction and a detailed study of the production reaction in nuclei. The elementary pion-production reaction relies on five Feynmann diagrams, which have N 's, Δ 's and N^* 's as intermediate isobars. The relative scattering amplitudes are derived from chiral lagrangian. The purely mesonic $\pi\pi$ amplitude is calculated by means of the coupled-channel Bethe–Salpeter equation. In the nuclear medium, the $(\pi\pi)_{I=J=0}$ interaction is strongly modified due to the coupling of pions to p - h and Δ - h excitations. This results in a displacement of the $\text{Im}T_{\pi\pi}$ strength toward the $2m_\pi$ threshold as the nuclear density increases. Conversely, the nuclear medium weakly affects the $(\pi\pi)_{I=2, J=0}$ interaction. The model includes several nuclear effects: Fermi motion, Pauli blocking, pion absorption and quasi-elastic scattering. The $\pi 2\pi$ process is found to occur at a mean nuclear density $\rho = 0.24\rho_n$ [16]. Finally, the model employs a Monte Carlo technique to generate and propagate $\pi 2\pi$ events, thus their phase space can easily accommodate the CHAOS acceptance.

(3) $\mathcal{M}3$: The work of Ref. [10] aims at studying the possibility of the σ -meson identification in nuclear matter, where the elusive particle might be detected as a consequence of the partial restoration of chiral symmetry. Due to the strong interaction of σ with the nuclear medium, the description of the σ properties in terms of parameters like m_σ and Γ_σ appears inadequate, and a proper observable becomes the σ spectral function. By using a simple but general approach, [10] proves that in the proximity of the $2m_\pi$ threshold the partial restoration of the chiral symmetry implies that the σ spectral function strength enhances as the σ total energy approaches $2m_\pi$. In order to render this general finding more quantitative, the theory uses the SU(2) lin-

ear sigma model, with the mean field correction in nuclear matter accounted for only by the leading diagram sketched in Fig. 2(b).

(4) $\mathcal{M}4$: This work [12] studies the $(\pi\pi)_{I=J=0}$ interaction in nuclear matter by constructing a microscopic theory for both the σ -meson propagator (D_σ) and the $\pi\pi$ T -matrices in the framework of the linear sigma model. In-medium pions are renormalized through their P -wave coupling to correlated p - h and Δ - h states (Fig. 2(a)). Bare sigmas, of the linear sigma model, are coupled to the nuclear medium via the diagram sketched in Fig. 2(b). The P -wave renormalization of sigmas leads to a downward shifts of the σ mass, which ultimately produces a strong enhancement of the σ -meson mass distribution (*i.e.* $\text{Im } D_\sigma$) around the $2m_\pi$ threshold. This enhancement is further increased by a factor of 2 to 3 by the S -wave renormalization of the bare σ -meson mass (*i.e.* by the partial restoration of chiral symmetry), which presents a similar behavior near the $2m_\pi$ threshold.

4. Results of the $\pi \rightarrow \pi\pi$ reaction in nuclei

A general property of the $\pi 2\pi$ process on nuclei in the low-energy $M_{\pi\pi}$ regime was outlined by previous experimental works: it is a quasi-free process both when it occurs on deuterium [17] and on complex nuclei [5]. Furthermore, a common reaction mechanism underlies the process whether it occurs on a nucleon or a nucleus [6]. Thus the study of the $\pi^+ {}^2\text{H} \rightarrow \pi^+ \pi^\pm NN$ reaction is dynamically equivalent to studying the elementary $\pi^+ n \rightarrow \pi^+ \pi^- p$ and $\pi^+ p \rightarrow \pi^+ \pi^+ n$ reactions separately.

4.1. The $\pi\pi$ invariant mass

Fig. 3 shows the single differential cross sections (diamonds) as a function of the $\pi\pi$ invariant mass ($M_{\pi\pi}$, MeV) for the two reaction channels $\pi^+ \rightarrow \pi^+ \pi^-$ and $\pi^+ \rightarrow \pi^+ \pi^+$. Horizontal error bars are not indicated since they lie within symbols. The $\pi A \rightarrow \pi\pi N[A-1]$ phase space simulations (dotted histograms) are also shown, and are normalized to the same area as the experimental distributions. Regardless of the nuclear mass number, the invariant mass distributions for the $\pi^+ \rightarrow \pi^+ \pi^+$ channel closely follow phase space, and the energy maximum increases with increasing A , that is, with increasing nuclear Fermi momentum. The $\pi^+ \rightarrow \pi^+ \pi^-$ channel displays a different behaviour. Compared to phase space, the ${}^2\text{H}$ invariant mass displays little strength from $2m_\pi$ to 310 MeV, while, in the same energy interval, the ${}^{12}\text{C}$, ${}^{40}\text{Ca}$ and ${}^{208}\text{Pb}$ $\pi^+ \pi^-$ invariant mass distributions increasingly peak as A increases. In order to explain the nature of the reaction mechanism contributing to the peak structure, it was useful to examine $\cos\Theta_{\pi\pi}^{\text{CM}}$ distributions (not shown) for those events with invariant masses $2m_\pi \leq M_{\pi^+\pi^-} \leq 310$ MeV. A partial wave expansion limited to the three

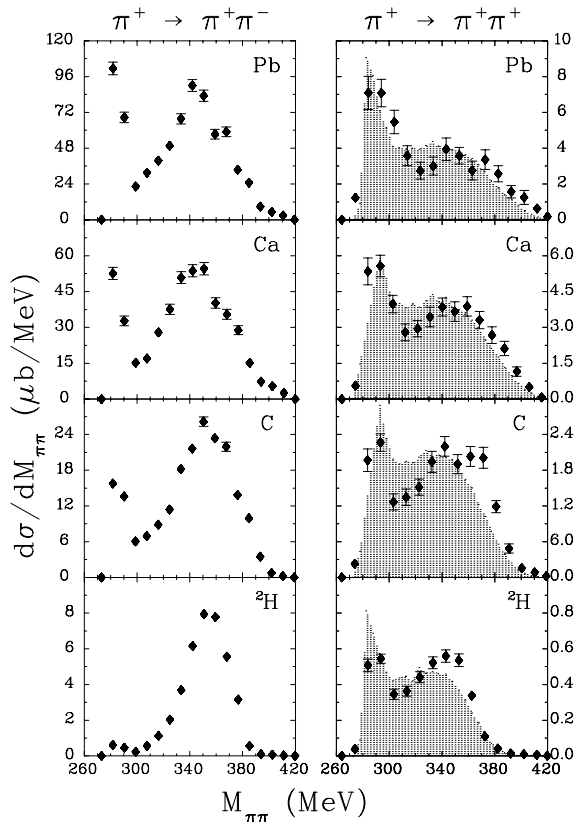


Fig. 3. Invariant mass distributions (diamonds) for the $\pi^+ \rightarrow \pi^+\pi^-$ and $\pi^+ \rightarrow \pi^+\pi^+$ reactions on ${}^2\text{H}$, ${}^{12}\text{C}$, ${}^{40}\text{Ca}$ and ${}^{208}\text{Pb}$. The shaded regions represent the results of phase-space simulations for the pion-production reaction $\pi A \rightarrow \pi\pi N[A - 1]$.

lowest waves, *i.e.* S , P and D was used to best-fit the $\Theta_{\pi\pi}^{\text{CM}}$ distributions. For all the nuclei studied $\chi_\nu^2 \leq 1$ which indicates that a proper number of waves was used in the expansion. In the case of heavier nuclei, the $\pi^+\pi^-$ system predominantly couples in S -wave $\sim 95\%$ (or $\ell = 0$) and a remaining 5% is spent in a D -wave ($\ell = 2$) state. Furthermore, within the sensitivity of the χ_ν^2 -method, any P -wave ($\ell = 1$) coupling of the two pions is excluded.

The results of two recent theoretical works, $\mathcal{M}1$ [11] and $\mathcal{M}2$ [9], which have modelled the $\pi\pi\pi$ reaction on nuclei, are reported in Fig. 4. The (short and long) dashed lines denote the $\mathcal{M}1$ calculations while the $\mathcal{M}2$ predictions are shown as full lines. In the case of Ca, $R1$ ($R2$) indicates the $\mathcal{M}1$ predictions for $\rho=0.7\rho_n$ ($\rho=0.5\rho_n$), while $V1$ is the result of the $\mathcal{M}2$ calculations for a mean $\rho=0.24\rho_n$. For the purpose of the present discussion, the curves in

Fig. 4 are normalized to the experimental data. For the $\pi^+ \rightarrow \pi^+\pi^+$ channel, the $R1$ and $R2$ distributions differ slightly from each other. The $R1$ distribution is broader, due to the larger nuclear Fermi momentum, which is a consequence of the higher nuclear density used [11]. The lower ρ used for $R1$ seems to describe the measured distribution better. This trend is also supported by $V1$ whose $\mathcal{M}2$ predictions agree well with the invariant mass distributions. Therefore, both $\mathcal{M}1$ and $\mathcal{M}2$ indicate that the average nuclear density of ^{40}Ca for which the production reaction takes place cannot exceed $0.5\rho_n$. In the $\pi^+ \rightarrow \pi^+\pi^-$ channel the distribution predicted by $\mathcal{M}2$ for ^2H is able to describe the data, thus placing the construction of nuclear medium effects on reliable grounds. The $\mathcal{M}2$ approach to ^{40}Ca includes Fermi motion, pion absorption, pion quasi-elastic scattering, and $(\pi\pi)_{I=J=0}$ medium modifications. Nevertheless, the model is unable to reproduce the observed $M_{\pi\pi}$ strength in the near threshold region. An increase of ρ from $0.24\rho_n$ to $0.5\rho_n$ and to $0.7\rho_n$ is unlikely to improve the agreement with the experimental cross section, see also Fig. 9 of Ref. [9]. In the case of $\mathcal{M}1$, the $R2$ prediction ($0.5\rho_n$) seems to reproduce the $M_{\pi\pi}$ distribution better, although some of the near-threshold yield already comes from the $\pi^+ ^2\text{H} \rightarrow \pi^+\pi^-pp$ production. The model, in fact, overestimates the cross

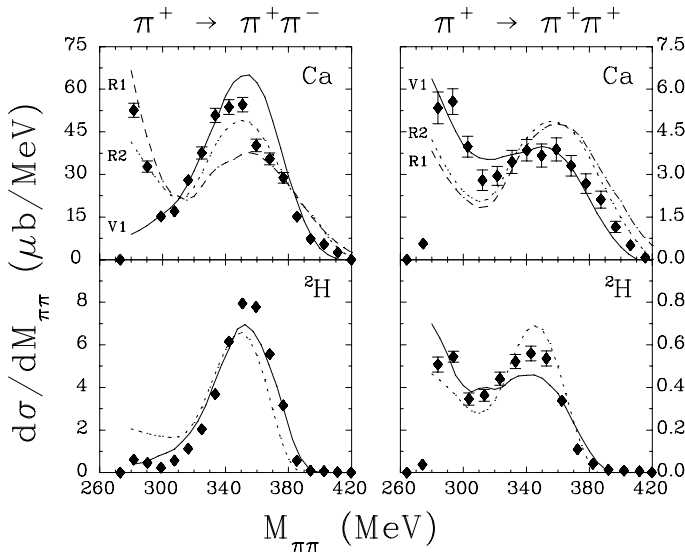


Fig. 4. Invariant mass distributions (diamonds) for the $\pi^+ \rightarrow \pi^+\pi^-$ and $\pi^+ \rightarrow \pi^+\pi^+$ reactions on ^2H and ^{40}Ca . The dashed curves are taken from Ref. [11] and the model is explained in $\mathcal{M}1$, $R1$ and $R2$ are the results for $0.7\rho_n$ and $0.5\rho_n$, respectively. The full curves ($V1$) are from the theoretical work of Ref. [9] $\mathcal{M}2$ with a mean $\rho = 0.24\rho_n$. The curves are normalized to the experimental data.

section at low invariant masses whose amount is shown in Fig. 4. The $R1$ solution ($0.7\rho_n$) provides the correct $M_{\pi\pi}$ near-threshold intensity but does not describe the remaining part of the distribution very well. Therefore, $V1$, $R1$ and $R2$ suggest that the missing $M_{\pi^+\pi^-}$ strength near the $2m_\pi$ threshold should be searched for in a stronger ρ -dependence of the $(\pi\pi)_{I=J=0}$ interaction, rather than by requiring the pion-production process to occur in an unlikely high-density nuclear environment.

4.2. The $\mathcal{C}_{\pi\pi}^A$ ratio

In this paragraph the observable $\mathcal{C}_{\pi\pi}^A$ is presented in comparison with recent theoretical predictions. $\mathcal{C}_{\pi\pi}^A$ is defined as the composite ratio $\frac{M_{\pi\pi}^A}{\sigma_T^A} / \frac{M_{\pi\pi}^N}{\sigma_T^N}$, where σ_T^A (σ_T^N) is the measured total cross section of the $\pi 2\pi$ process in nuclei (nucleon). This observable has the property of yielding the net effect of nuclear matter on the $(\pi\pi)_{I=J=0}$ interacting system regardless of the $\pi 2\pi$ reaction mechanism used to produce the pion pair [6]. Therefore, $\mathcal{C}_{\pi\pi}^A$ can be compared not only with the $\mathcal{M}1$ and $\mathcal{M}2$ predictions which explicitly calculate both $M_{\pi\pi}^{\text{Ca}}$ and $M_{\pi\pi}^{2\text{H}}$, but also with the theories described in $\mathcal{M}3$ and $\mathcal{M}4$ because they calculate the mass distribution of an interacting $(\pi\pi)_{I=J=0}$ system (*i.e.* $\text{Im} D_\sigma$) both in vacuum and in nuclear matter. Since the calculations are reported either in arbitrary units [9,11] or in units which are complex to scale [10,12], theoretical predictions are normalized to the experimental distributions at $M_{\pi\pi} = 350 \pm 10$ MeV, where the $\mathcal{C}_{\pi\pi}^A$ distribution is flat.

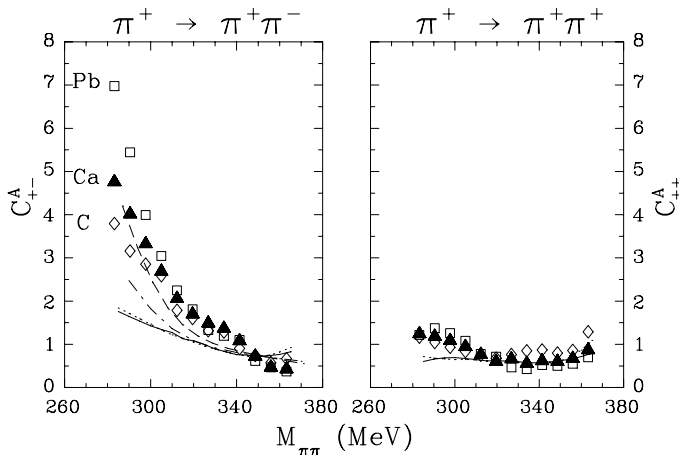


Fig. 5. The composite ratios $\mathcal{C}_{\pi\pi}^A$ for ^{12}C , ^{40}Ca and ^{208}Pb . The curves are taken from [9] (full) and the model is described in $\mathcal{M}2$, [10] (dash-dotted) $\mathcal{M}3$, [11] (dotted) $\mathcal{M}1$ and [12] (dashed) $\mathcal{M}4$. Further details are reported in the text.

For both reaction channels, the full [9] and dotted [11] curves in Fig. 5 are obtained by simply dividing $M_{\pi\pi}^{\text{Ca}}/M_{\pi\pi}^{2\text{H}}$. It is worthwhile recalling that for [11] the option $\rho = 0.5\rho_n$ is used while for [9] $\rho = 0.24\rho_n$. Furthermore, for both approaches the underlying medium effect is the P -wave coupling of π 's to p - h and Δ - h configurations, which accounts for the near-threshold enhancement. When applied to the $\mathcal{C}_{\pi\pi}^{\text{Ca}}$, both $\mathcal{M}1$ and $\mathcal{M}2$ predict the same result, which describes the behaviour of $\mathcal{C}_{++}^{\text{Ca}}$ fairly well throughout most of the $M_{\pi\pi}$ energy range, but only reproduces a small part of the near-threshold strength for $\mathcal{C}_{+-}^{\text{Ca}}$. $\mathcal{M}3$ [10] and $\mathcal{M}4$ [12] examine the medium modifications on the scalar-isoscalar meson, the σ -meson. Nuclear matter is assumed to partially restore chiral symmetry, and consequently m_σ is assumed to vary with ρ . The variation is parametrised as $1 - p(\rho/\rho_n)$, where is $p = 0.2$ and $\rho = \rho_n$. The choice $\rho = \rho_n$ may result appropriate for ^{208}Pb but it is not for medium (*i.e.* ^{40}Ca) and light (*i.e.* ^{12}C) nuclei. In Fig. 5 the predictions of $\mathcal{M}3$ and $\mathcal{M}4$ are shown as the dash-dotted curves and dashed curves, respectively. $\mathcal{M}4$ predicts a larger near-threshold strength, which is due to the combined contributions of the in-medium P -wave coupling of pions to p - h and Δ - h configurations, and to the partial restoration of chiral symmetry in nuclear matter. These two models, however, are still too schematic for a conclusive comparison to the present data, and full theoretical calculations are called for.

5. Existing $\pi 2\pi$ results

Novel $\pi 2\pi$ results [18] were recently presented by the Crystal Ball (CB) Collaboration at the AGS. The $\pi^- A \rightarrow \pi^0 \pi^0 A'$ production reaction was studied on H, ^{12}C , ^{27}Al and ^{64}Cu at $T_{\pi^-} = 291.6$ and 623.3 MeV. The figures presented in Ref. [18], however, are only for the results obtained at the higher energy. The $M_{\pi^0 \pi^0}^A/M_{\pi^0 \pi^0}^C$ ratio in Ref. [18] has marked similarities to the observable $\mathcal{C}_{\pi^+ \pi^-}^A$. Namely, the two ratios are flat at around 400 MeV invariant mass but increase as $M_{\pi\pi}$ approaches the $2m_\pi$ threshold, and, near threshold, both ratios increase as A increases. Unlike the CHAOS data, the invariant mass distributions in [18] show no evidence of a peak at the $2m_\pi$ threshold. However, the CB and CHAOS spectra do share relevant features: they both have meager $M_{\pi\pi}$ strength near threshold for H (^2H for CHAOS), and show a dramatic increase of strength with increasing A .

6. Conclusions

In this article the results of an exclusive measurement of the $\pi^+A \rightarrow \pi^+\pi^\pm A'$ reactions on ${}^2\text{H}$, ${}^{12}\text{C}$, ${}^{40}\text{Ca}$, and ${}^{208}\text{Pb}$, at an incident pion energy $T_{\pi^+} = 283$ MeV, were presented. The primary interest was directed to the study of the $\pi\pi$ -dynamics in nuclear matter.

$\mathcal{C}_{\pi\pi}^A$ was found to yield the net effect of nuclear matter on the $\pi\pi$ system regardless of the $\pi 2\pi$ reaction mechanism used to produce the pion pair. These distributions display a marked dependence on the charge state of the final pions. The $\mathcal{C}_{\pi^+\pi^-}^A$ distributions peak at $2m_\pi$ and their yield increases as A increases, thus indicating that pion pairs form a strongly interacting system. Furthermore, the $\pi\pi$ system couples to $I = J = 0$, the σ -meson channel. In the $\pi^+ \rightarrow \pi^+\pi^+$ channel, the $\mathcal{C}_{\pi\pi}^A$ distributions show little dependence on either A or T , thus indicating that nuclear matter only weakly affects the $(\pi\pi)_{I,J=2,0}$ interaction. The $\mathcal{C}_{\pi^+\pi^-}^A$ observable was compared with theories which included the $(\pi\pi)_{I=J=0}$ in-medium modifications associated with the partial restoration of chiral symmetry in nuclear matter, and with model calculations which only included standard many-body correlations, *i.e.* the P -wave coupling of π' s to p - h and Δ - h configurations. It was found that both mechanisms are necessary to interpret the data.

Monte Carlo simulations of the $\pi^+A \rightarrow \pi^+\pi^\pm N[A-1]$ reaction phase space proved useful in the interpretation of some of the $\pi 2\pi$ data. In the case of $M_{\pi^+\pi^+}$, the distribution of $\pi^+\pi^+$ pairs follows phase space. For the $M_{\pi^+\pi^-}$ distributions, the $\pi\pi$ dynamics overwhelms the dipion kinematics. Unlike the phase space simulations, the near-threshold $\pi^+\pi^-$ yield is suppressed in the elementary production reaction, $\pi^+ {}^2\text{H} \rightarrow \pi^+\pi^- pp$ in the present work, while, in the same energy range, medium modifications strongly enhance $M_{\pi^+\pi^-}$. Any interpretation of the shape of the $M_{\pi^+\pi^\pm}^A$ (or $\mathcal{C}_{\pi^+\pi^\pm}^A$) distributions should combine the effects of the restoration of chiral symmetry in nuclear matter, and standard many-body correlations. Such an approach would not require a high-density nuclear medium to obtain strong $\pi\pi$ medium modification in the proximity of the $2m_\pi$ threshold. The results of the present measurement were compared with results from the Crystal Ball Collaboration at the BNL, which are the only relevant ones available. The exclusive $\pi 2\pi$ CB measurement independently confirms that the nuclear medium strongly influences the $\pi\pi$ interaction in the $I = J = 0$ channel.

REFERENCES

- [1] F. Bonutti *et al.*, *Nucl. Phys.* **A638**, 729 (1998).
- [2] M. Kermani *et al.*, *Phys. Rev.* **C58**, 3419 (1998).

- [3] M. Kermani *et al.*, *Phys. Rev.* **C58**, 3431 (1998).
- [4] F. Bonutti *et al.*, *Phys. Rev. Lett.* **77**, 603 (1996).
- [5] F. Bonutti *et al.*, *Phys. Rev.* **C55**, 2998 (1997).
- [6] F. Bonutti *et al.*, *Phys. Rev.* **C60**, 018201 (1999).
- [7] P. Schuck W. *et al.*, *Z. Phys.* **A330**, 119 (1988); G. Chanfray *et al.*, *Phys. Lett.* **B256**, 325 (1991); P. Schuck *et al.*, 36th International Winter Meeting on Nuclear Physics, Bormio, Jan. 1998.
- [8] H.C. Chiang *et al.*, *Nucl. Phys.* **A644**, 77 (1998).
- [9] M.J. Vicente-Vacas *et al.*, *Phys. Rev.* **C60**, 064621 (1999).
- [10] T. Hatsuda *et al.*, *Phys. Rev. Lett.* **82**, 2840 (1999), and references therein quoted.
- [11] R. Rapp *et al.*, *Phys. Rev.* **C59**, R1237 (1999).
- [12] Z. Aouissat *et al.*, nucl-th/9908076 v2 31 Aug 1999; D. Davesne *et al.*, nucl-th/9909032 15 Sept 1999.
- [13] G.R. Smith *et al.*, *Nucl. Instrum. Methods Phys. Res.* **A362**, 349 (1995).
- [14] F. Bonutti *et al.*, *Nucl. Instrum. Methods Phys. Res.* **A350**, 136 (1994);
- [15] R. Rapp *et al.*, *Phys. Rev.* **A596**, 436 (1996).
- [16] M.J. Vicente-Vacas *et al.*, nucl-th/0002010 Feb. 2000.
- [17] R. Rui *et al.*, *Nucl. Phys.* **A517**, 445 (1990); C.W. Bjork *et al.*, *Phys. Rev. Lett.* **44**, 62 (1980); J. Lichtenstadt *et al.*, *Phys. Rev.* **C33**, 655 (1986); V. Sossi *et al.*, *Nucl. Phys.* **A548**, 562 (1992).
- [18] B.M.K. Nefkens, Eighth International Symposium on Meson-Nucleon Physics and the Structure of the Nucleon, Zuoz (Switzerland) Aug 15-21, 1999, published by π NNEWSLETTER No. 15 78 (1999).